MLI Impact Phenomenology Observed on the HST Bay 5 MLI Panel

Melissa A. Ward [(1)] and Phillip D. Anz-Meador [(1)]

[(1)] Jacobs, NASA Johnson Space Center, Mail Code XI5-9E, 2102 NASA Parkway, Houston, TX 77058, USA, melissa.a.ward@nasa.gov, phillip.d.anz-meador@nasa.gov

ABSTRACT

Multi-layer insulation (MLI) blankets covering the Hubble Space Telescope (HST) electronics bays were removed during HST Servicing Mission 4 and returned to Earth for analysis. The NASA Orbital Debris Program Office obtained HST Bay 5, 8, and 10 MLI blankets to characterize impact features and develop a flux estimate based on those features. This paper reports on the impact feature phenomenology observed during imaging campaigns in 2011 and 2018. Earlier conventions of measuring impacted features by recording the largest diameter to determine impacting particle size do not provide the best subsequent estimation of the impacting particle size. Instead of an impacted feature as a smooth-edged through-hole, a 'petaling' phenomenon along with multiple-layering composition in impacted features has been observed in both hypervelocity testing and in the Bay 5 MLI. A new methodology of characterization techniques used during research and analysis of the HST MLI is presented, which will provide greater understanding and a more accurate estimation of impacting particles and their parameters.

1 INTRODUCTION

Approximately 80% of the Hubble Space Telescope's (HST) external surfaces are covered with thermal tape or multi-layer insulation (MLI) blankets to protect against the space environment thermal changes. Servicing missions 1-4 conducted extra vehicular human inspections, as well as photographic inspections of the exterior for the purposes of assessing space environment weathering and spacecraft health. Damage to MLI blankets on electronics bays 5, 8 and 10 were previously assessed and repairs and replacements were conducted during extra vehicular activities. The original MLI blankets, now returned to the ground, provide a useful source of high-altitude impact data due to their long duration, area, and placement on the HST. The Orbital Debris Program Office (ODPO) uses the returned MLI blanket's impact feature morphology to better understand and model the small, penetrating micrometeoroid and orbital debris (MMOD) environment. The 2018 survey at JSC reveals complex, impact feature phenomena on the blankets, requiring effort to characterize, measure, and interpret feature morphology. Techniques used to characterize, measure, and interpret the impact features, facilitating Orbital Debris Engineering Model (ORDEM) 3.1 validation, are described.

2 BACKGROUND

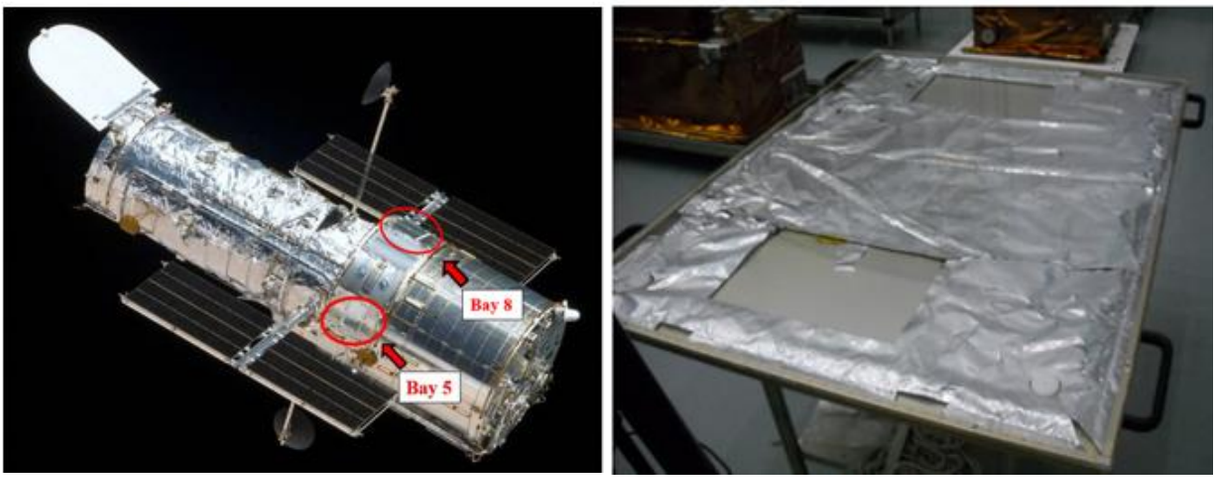

Fig. 1. Left: Bays 5 and 8 locations on the HST. Right: Bay 5 MLI blanket at GSFC after return from orbit.

MLI blankets for HST electronics bays 5, 8, and 10 were retrieved by servicing mission 4/ (Space Transportation System (STS)-125) in 2009 and returned to Earth. Bays 5 and 8 had been exposed to the space environment for approximately 19 years,

whereas Bay 10 had been exposed for 9.8 years. After examination by other project teams, MLI blankets from bays 5 and 8 were delivered to ODPO for detailed inspection. Blankets consist of a 17-layer MLI stack of 5 mil (127 μm) thick vapor deposited Aluminum (VDA)-Teflon outer layers and 15 0.3 mil (7.62 μm) VDA-Kapton inner layers. The utility of Bay 8 was lessened by the removal of the majority of the outer exposed blanket layer by prior unassociated projects, so the work reported in this paper concerns Bay 5 exclusively.

Three surveys have been conducted on the Bay 5 MLI blanket at Goddard Space Flight Center (GSFC) and Johnson Space Center (JSC). The first GSFC 2009 survey inspected impact features of approximately 400 μm and larger, and the JSC 2011 survey inspected features of approximately 100 μm and larger. The initial JSC 2018 survey motivation was a requirement to validate ORDEM 3.1, currently in final review for public release, at altitudes above the International Space Station and human spaceflight. The HST's WFPC-2 and MLI cratering records offer a means to facilitate validation. The JSC 2011 survey outcomes were reviewed, and certain deficiencies were noted. Crater features were not characterized and through-holes were only complete for sizes larger than 100 μm. A previously surveyed larger area had been excised from the blanket by other analysis teams and thus was no longer available for examination. The 2011 feature survey used a prior-generation VHX-600 Keyence digital microscope but did not employ backlighting, which led to some incorrect measurements of feature size being detected when reexamined in the 2018 survey; this was considered sufficient to invalidate the 2011 survey. Given that a current-generation VHX-5000 was available, as well as newly developed feature identification and characterization aides, Sample #1 was resurveyed. To decrease Poisson sampling uncertainties by a factor of two, three additional 20×20 cm samples were cut from the top layer of Bay 5 MLI. Figure 2 identifies the sample locations with the tally of through-holes and craters for each sample.

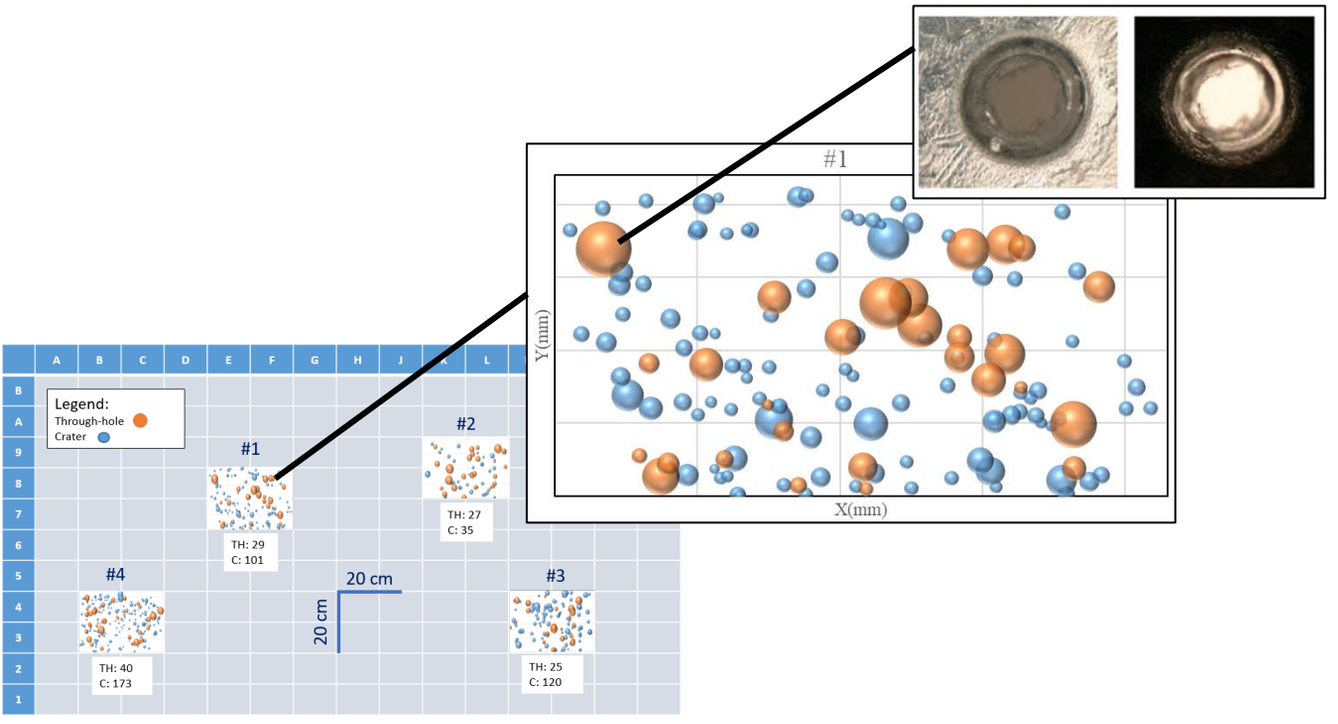

Fig. 2. Left: Bay 5 MLI grid square coordinate system and the four 20×20 cm samples discussed in this paper. Each grid square is 10 cm on a side; grid rows are denoted as 1-B and grid columns A-Q. A given square is identified by column and row, and multi-square areas are identified by the lower left-upper right diagonal grid square identifiers. For example, the lower left grid square is A1. The total number of through-holes (TH) and craters (C) are listed for each sample.
Middle pop out: Enlarged locations of impact features for Sample #1. Pop out right: Front-lit example of a through-hole. Right: Backlit example of same through-hole.

Based on ground-based testing [1], clean through-holes in the MLI would be expected for projectile size-to-MLI outer layer thickness (d_p/T) ratio > 30. As this would correspond to projectile diameters on the order of 4 mm, clean holes were not expected. HST MLI through-hole impact features were observed to display a jagged or petaled innermost opening as well as terracing, looking inward on the feature. This phenomenon was seen in the Solar Max satellite inspection [2], the HST solar

arrays, the European Retrievable Carrier [3], and in hypervelocity testing of through-holes in variable thicknesses [4]. However, no further research concerning impact feature morphologies themselves has been identified by the project team. The observed phenomenon creates uncertainty when measuring feature size. In fact, several measurement could possibly be considered indicative of the true projectile size. This required detailed investigation.

3 Impact Feature Characterization

An impact feature's shape, size, depth, and volume were recorded for each 20 cm-square sample. The VHX-5000 is a digital microscope manufactured by Keyence, used in the ODPO to evaluate the properties of a material, component, or system without causing damage or destroying the serviceability of the material. Through-holes and numerous impact craters greater than 10 μm were documented using the VHX and a motorized gantry with programmed joystick. On the gantry was an LED light pad that permitted back lighting of impact features. An X/Y coordinate plane was projected on each sample to allow locating impact features post inspection and to track impact feature morphology throughout each layer of the blanket stack. During inspection, there was difficulty in determining through-hole or crater impact-feature boundaries visually as the backlight would appear to blend into a feature, as demonstrated by Fig. 4's left-most images. Commercially available color filter gels were used to increase contrast and better reveal morphological borders for identification and characterization.

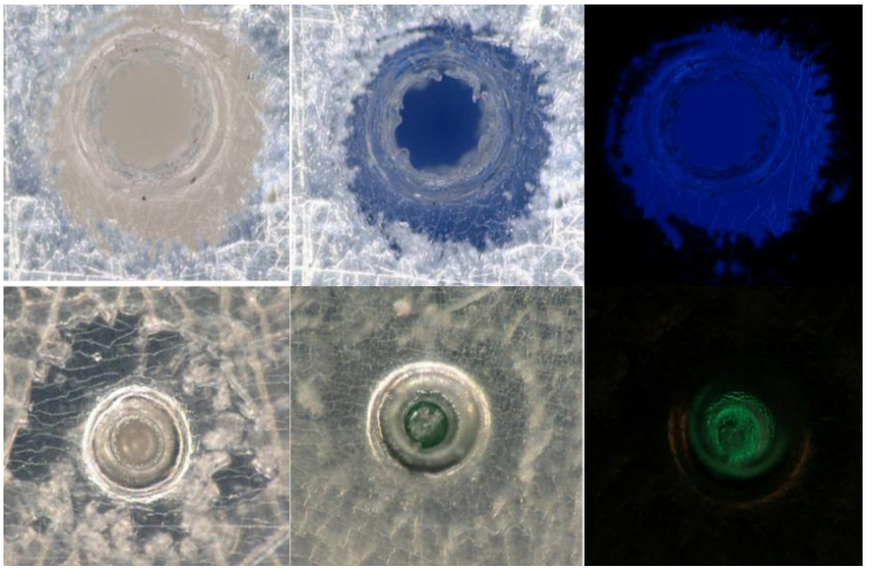

Fig. 4. From left to right: Basic front-lit photo of impact features (before blue and green filters to enhance contrast are applied), front-lit photo after filters are applied, and back-lit photos after filters are applied.

Even with filtering techniques, measuring feature diameter is difficult, as there is often no well-defined or clear through-hole, or confusing multiple features may be present. The relationship of feature diameter to projectile size is a ratio depending on thickness of material, so simply using the largest diameter measurement may not return the best estimation of projectile size For circular impact features, diameters were recorded; for elliptical impact features both major and minor axis diameters were recorded. When an impact feature shape did not fit into these two categories, the largest diameter was recorded. Common characteristics were observed with sufficient regularity that a taxonomy of HST MLI morphological features could be defined. Definitions can also change based on the observers' specific lighting configuration. Front lit configurations are those where light is projected onto the front of the impact feature by the VHX microscope. Back lit configurations are those where the light is projected from behind the impact feature by the LED light pad. Examples of both configurations are presented in Fig. 4 and Fig. 5. All measurements discussed in this paper were taken in a front-lit configuration.

To assist in identifying areas for measurement, an overhead view of a spherical impact identifying taxonomic measurements is shown in Fig. 5. The two innermost diameters are called the inner through-hole (ITH) and outer through-hole (OTH). Two measurements are taken here to allow for ripping effects. Going outward, the opaque erosion zone (OEZ) is seen as a partially see-through ring (hypothesized to be the target material "eroding" away). The transmission zone (TZ) is identified as a ring of light (coming in from the lighting pad). The inner coating melt (ICM) and outer coating melt (OCM) form the lip of the impact feature, and the diameter beyond the raised lip segues into the target material's nominal surface plane.

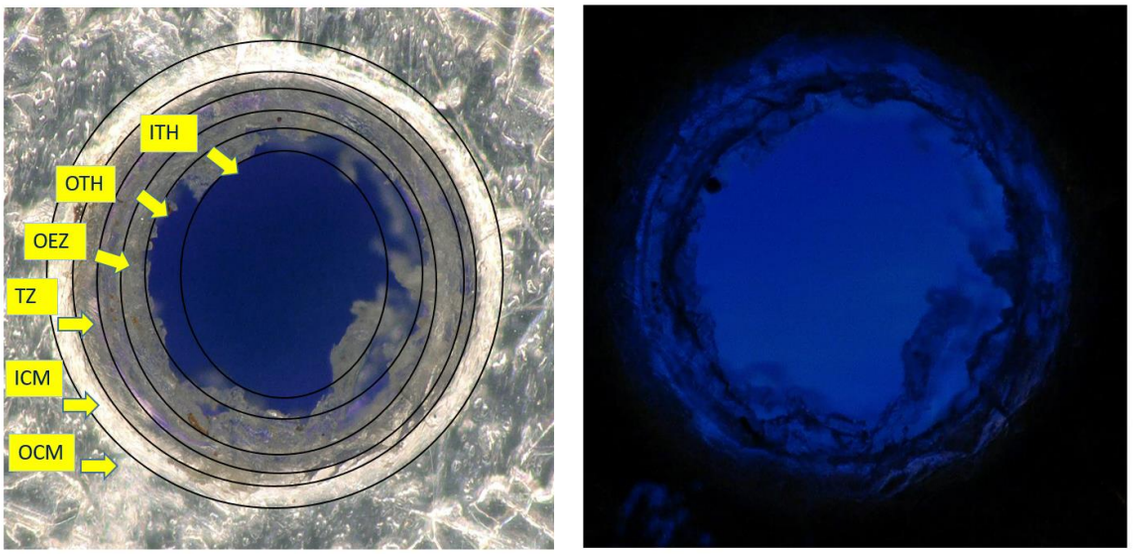

Fig. 5. Left: Feature nomenclature in a front-lit configuration. Right: Same through-hole feature in a back-lit configuration.

3.1 Cross Section Imaging

To better understand some of the features and taxonomic boundaries or areas identified in overhead imaging, the VHX microscope was used to construct a three-dimension (3D) depth composition of select penetrations and craters. To represent the depth composition of an impact feature, the VHX digital microscope scans through the focal range/sample depth trade-space in finite steps and builds a fully focused image. The small depth of field on the microscope allows multiple focused images at different depths to build a "depth profile," a non-destructive cross sectional view. However, the microscope profiling can be limited or compromised by the depth or bottom of the impact feature, specular features, discontinuous features and/or high rate-of-change features such as impact feature walls. For example, in the 3D cross section image, the petaling phenomenon observed from overhead imaging was not detected; instead, the microscope presented a flat bottom (Fig. 6 bottom).

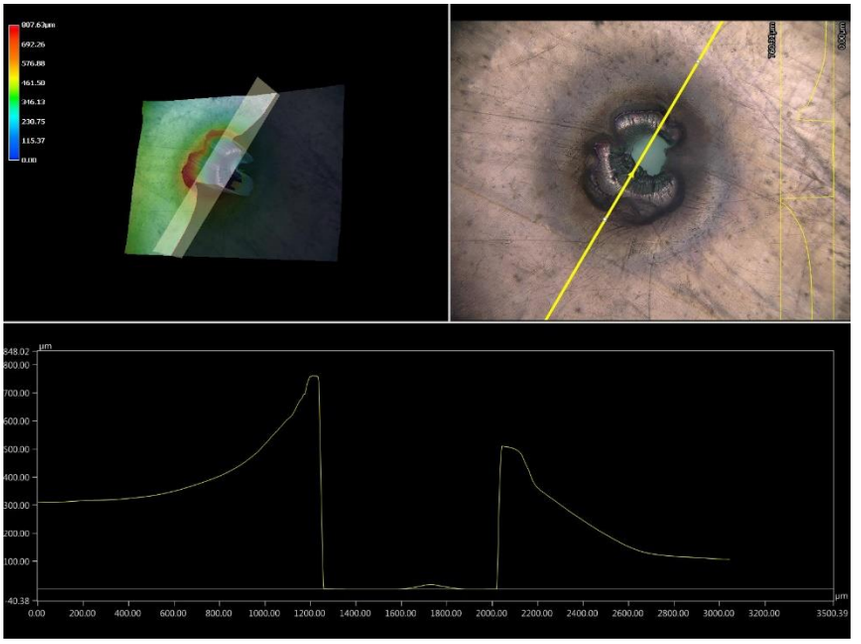

Fig. 6. Top: Overhead view of a through-hole. Bottom: VHX 3-D image profile of through-hole.

To better resolve morphological phenomena observed in overhead inspection while mitigating the limitations of the VHX depth composition, a Focused Ion Beam (FIB) was used to cross-section two additional through-holes and a crater collected from the

edges of the Bay 5 blanket. Impact feature regions were matched to crater profile imagery (Fig.7). The FIB imagery does not show strong terracing as implied by the depth composition. It is possible some impact features (*i.e.*, terracing) from overhead imaging are artifacts of the VHX onboard image analysis and depth composition. Figure 8 examines a through-hole cross section and an FIB image of corresponding areas of interest. While the terracing is not observed in practice, the petaling phenomenon is clearly observed.

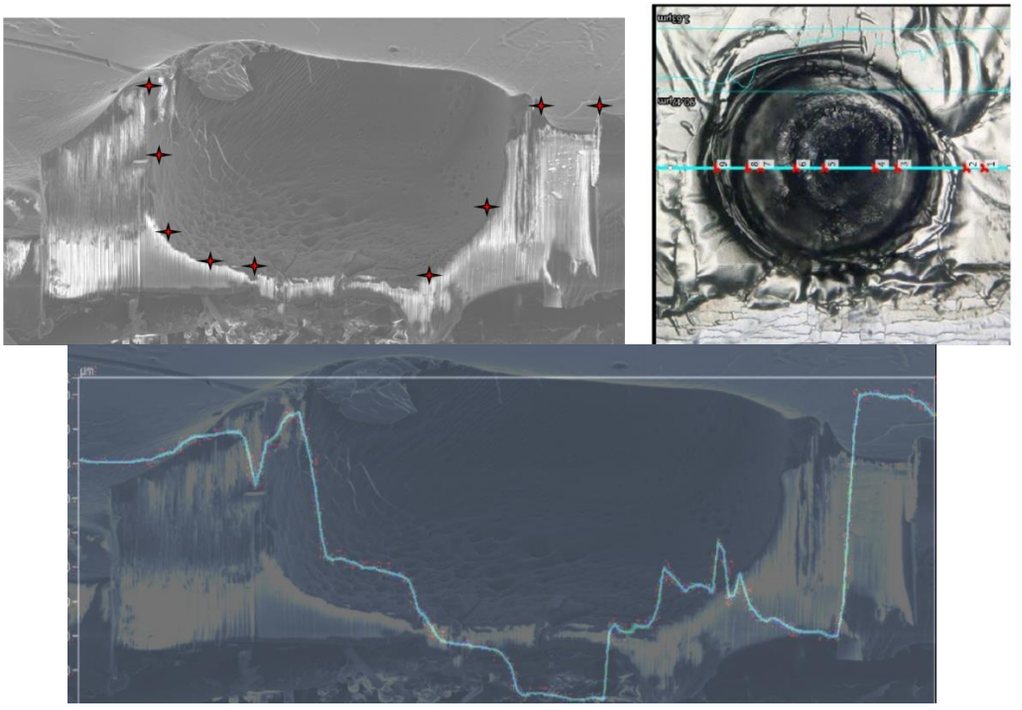

Fig. 7. Right: FIB crater cross section with corresponding sections on overhead photo.
Bottom: VHX 3D profile overlain on the FIB microphotograph.

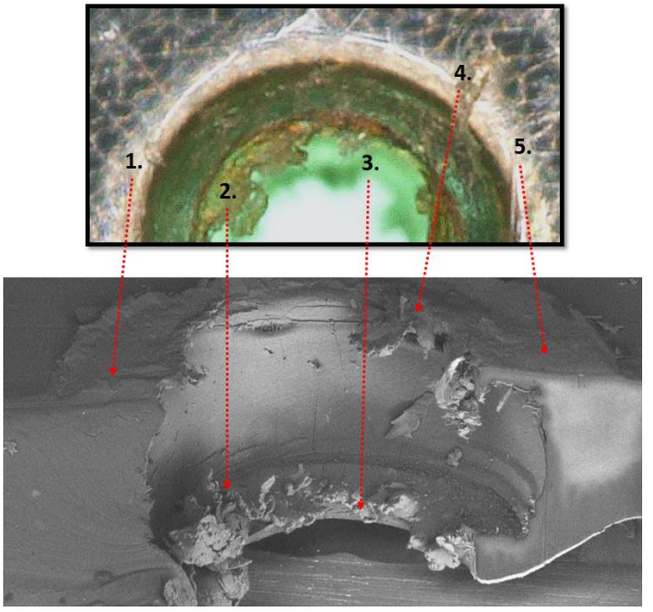

Fig. 8. Overhead cross section image of a through-hole with corresponding locations of interest on FIB cross section image. Numbers 1 and 5 indicate the lips of the through-hole, while 2, 4, and 3 indicate the jagged, petaled target material being observed at different depths.

3.2 Observational Findings

For all four samples and their layers, 550 features were identified. For the first layer, through-hole diameters ranged from 26 µm to 853 µm and crater sizes ranged from 9 µm to 537 µm. Over all samples, Layer 1 had 121 through-holes and 429 craters total. A detailed summary of the diameter ranges and count of features for each layer is presented in Table 1. Impact features also changed size and shape through each layer. Some impact features were observed through 8 of the 17 layers. No impact features made it completely through the 17 layer stack. The second layer (which is a much thinner material than the outer layer) displayed smooth, rather than petaled, through-holes (Fig. 9).

Table 1. Through-hole and crater count and diameter ranges for all samples and layers.

Samples 1-4	Feature Count							
Diameter Range (um)	Layer 1	Layer 2	Layer 3	Layer 4	Layer 5	Layer 6	Layer 7	Layer 8
<100	395	6	1	1	0	0	0	0
101-200	89	2	2	0	0	0	0	0
201-300	30	1	0	0	0	0	0	0
301-400	20	5	0	0	0	0	0	0
401-500	7	2	2	0	0	0	0	1
501-600	3	4	1	2	1	1	0	0
601-700	1	2	1	2	0	0	0	0
701-800	4	3	2	0	0	0	0	0
801-900	1	2	0	1	0	0	0	0
>901	0	6	12	4	2	2	2	0
Total Features	550	33	21	10	3	3	2	1
Through-Holes	121	19	9	3	3	1	1	0
Craters	429	14	12	7	0	2	1	1

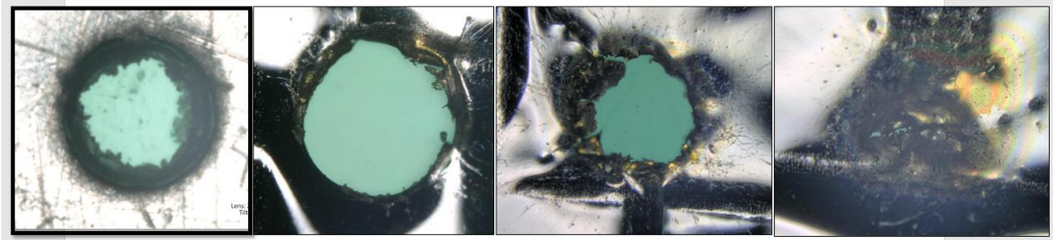

Fig. 9. Impact projectile pattern through top and first three inner blanket layers. Note that the third innermost layer displays multiple, very small impact crater features analogous to certain multi-shock shields or witness plates.

The cumulative number density as a function of observed feature diameter was plotted (Fig. 10) to determine if a specific point exists for the sizes where a projectile penetrates (through-hole) versus only cratering (non-penetration). Top/outer layer blanket thickness (127 µm) is also identified in Figure 10. There is an intersection of penetration and non-penetration features around 100 µm, where the craters dominate the through-holes at sizes less than 100 µm. Note however, the presence of many large crater features.

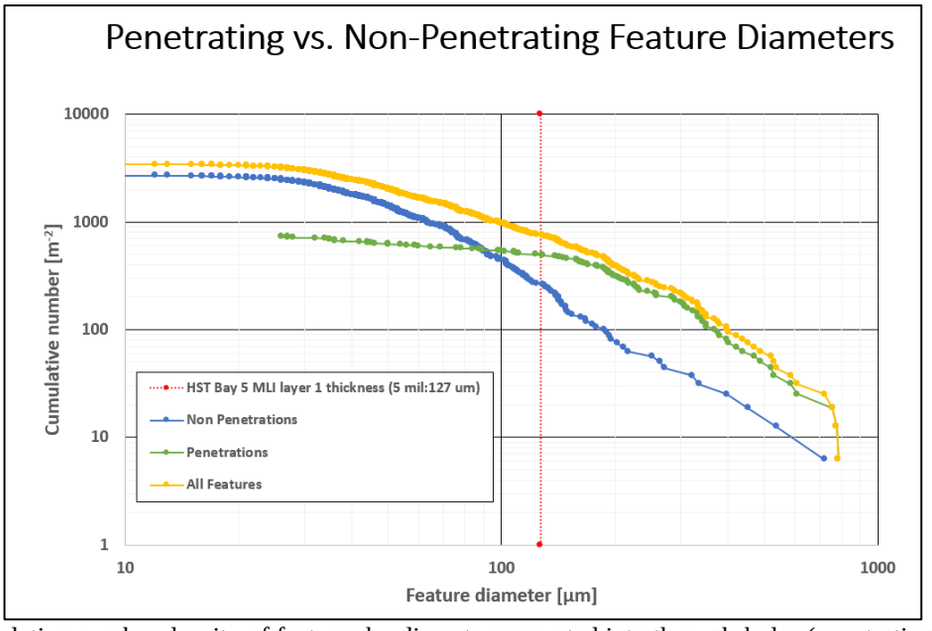

Fig. 10. Cumulative number density of features by diameter separated into through-holes (penetrating) and craters (non-penetrating). Diameter for elliptical features was the semi-minor diameter, which accounted for potentially oblique impact effects.

The 2018 survey is considered complete to the 26 µm-limiting penetration feature size, as revealed by backlighting. Non-penetrating impact features are estimated to be complete to 40–50 µm for samples 1, 3, and 4, and approximately 80 µm for sample 2. These larger limiting sizes for non-penetrating features are due primarily to challenges in feature identification at a magnification of 200X.

4 HYPERVELOCITY TESTING TO FACILITATE IN-SITU DATA INTERPRETATION

The NASA JSC Hypervelocity Impact Technology (HVIT) group conducted extensive impact testing at NASA White Sands Test Facility (WSTF) in U.S. Fiscal Year 2010 to formulate appropriate damage equations for HST coated surfaces (*e.g.*, the WFPC-2 radiator), MLI, and silver thermal tape (as used on the HST bus and optical tube). Damage equations relate known projectile size and launch criteria to observed target damage. The HVIT WSTF campaigns comprised a total of seven tests (six successful) launching medium (soda lime glass and Al 2017-T4 alloy) and high (Nickel) mass density spherical projectiles at a single-layer MLI material similar to the HST outer/top MLI blanket material. Similar penetration features were observed in the WSTF 2010 testing impact features and HST MLI blanket impact features (Fig. 11). Derivation of MLI damage equations at the time was deferred by higher-priority tasking and resource allocation and availability. The formulation of an MLI damage equation to support the 2018 survey is described in Section 5.

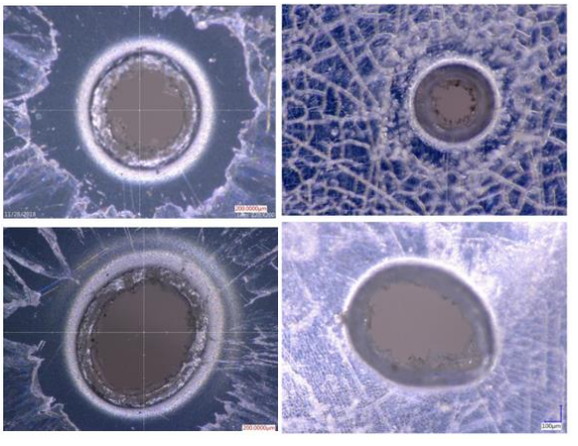

Fig. 11. Left: HVIT 2010 WSTF impact feature petaling. Right: HST MLI impact features with similar petaling.

5 QUANTITATIVE CHARACTERIZATION

With no known standard relationship linking craters/through-holes and their transition point, through-holes and craters are further investigated separately. Additionally, there is no known cratering damage equation, so craters are deferred until more research is complete. All results using laboratory-derived impact damage equations use through-hole data only. A generic damage equation (1) is used:

$$d_h = c * \boldsymbol{d}_p^{\alpha} * \rho_p^{\beta} * (v\cos\theta)^{\gamma}, \quad (1)$$

where d_h (the diameter of the impact hole) and d_p (the projectile diameter) are in millimeters, and ρ_p (the projectile density) is in grams per cubic centimeter. The velocity of the projectile (v) is measured in kilometers per second. The angle at which the projectile impacts (θ) is in degrees. The factor c and the exponent ensemble α, β, and γ are to be estimated. Using given parameters (projectile density, diameter, mass, velocity, and angle) from the HVIT 2010 WSTF campaign, and the same measurement techniques used with HST MLI blankets, diameter measurements (ITH, OTH, and OCM) of impact features are recorded for test shots. Exponents for the generic damage equation were estimated by the least squares (best-fit) method. These exponents were calculated for ITH, OTH, and OCM diameter measurements with the intent of determining which measurement diameter produces the least error for estimating feature diameter. The 'Feature Predicted Diameter' estimate versus 'Feature Actual Diameter' comparison is plotted in Fig. 12. The OTH measurements provide the least amount of error. The calculated exponents for the three diameters and their percent error of estimated versus actual diameter measurements are available in Table 2. The generic damage equation was inverted to allow prediction of projectile diameter from the given test data. Again, the OTH measurement produced the lowest error from actual measurement.

Table 2. Calculated exponent values for the generic damage equation and their resulting error percent of estimated versus actual diameter measurement. These exponents were calculated for ITH, OTH, and OCM measurements.

Calculated exponents	C	α	β	γ	Error % Estimated vs. Actual Feature Diameter	Error % Estimated vs. Actual Projectile Diameter
ITH	0.979	0.954	0.281	0.204	2.76	0.14
OTH	0.991	0.866	0.293	0.196	1.96	0.17
OCM	1.22	0.611	0.131	0.269	9.44	0.13

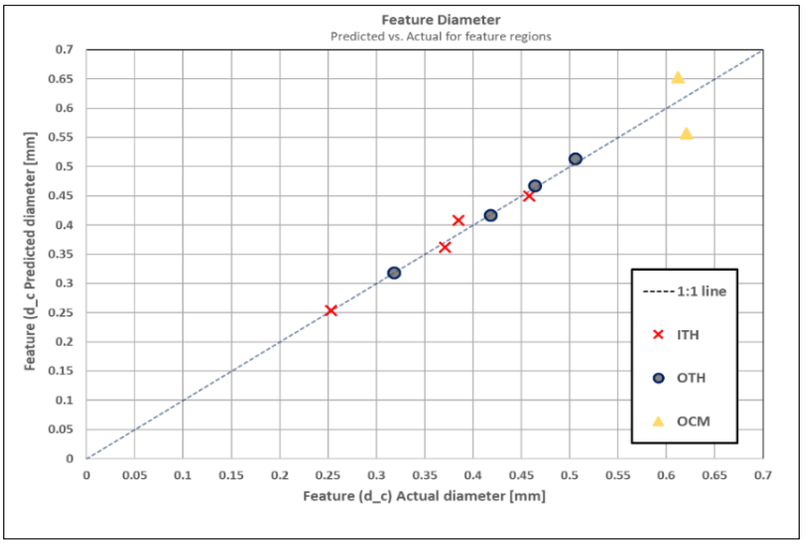

Fig. 12. Predicted impact feature diameter and HVIT test actual impact feature diameter correlation.

The inverted damage equation predicted projectile size for all of the OTH measurements in the MLI blanket samples. These are portrayed in Fig. 13, referenced to the thickness of the MLI top layer, and agnostic in terms of mass density—the two curves are for all medium density (2.8 g/cm^3 for evaluation) and high density (7.9 g/cm^3 for evaluation). The size estimate further incorporates HST attitude time histories for Bay 5 MLI over its total exposure time to better estimate the velocity and angle dependencies in Eq. 1, and represents the average size of ORDEM size bins.

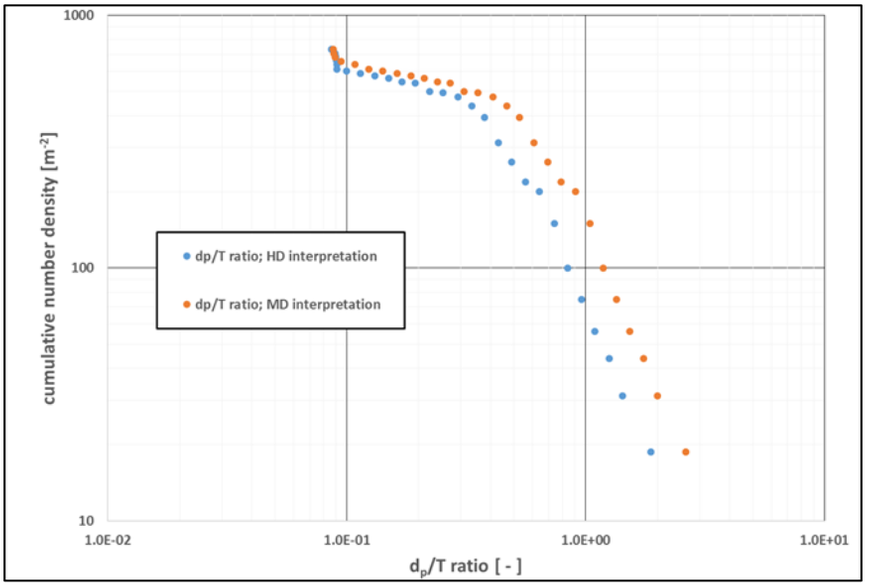

Figure 13. The cumulative number density as a function of the ratio of estimated projectile diameter to MLI outer blanket thickness T (5 mil/127 μm).

Significant inflection of the interpreted d_p is apparent at d_p/T values > 0.4-0.5 (depending upon mass density), which appears to be generally consistent with prior work generated in ground-based testing facilities [5] and indicative of a transition from cratering to attached spall, to detached spall, to full penetration of the target. This lends additional credence to the current interpretive damage equations and measurement methodologies. The size ensembles for both total MD and HD interpretation were used in validating the ORDEM 3.1 model [6]. This comparison offered good agreement between the MLI impact record and ORDEM 3.1, and a significantly better agreement when compared with the legacy ORDEM 3.0 (Fig. 14).

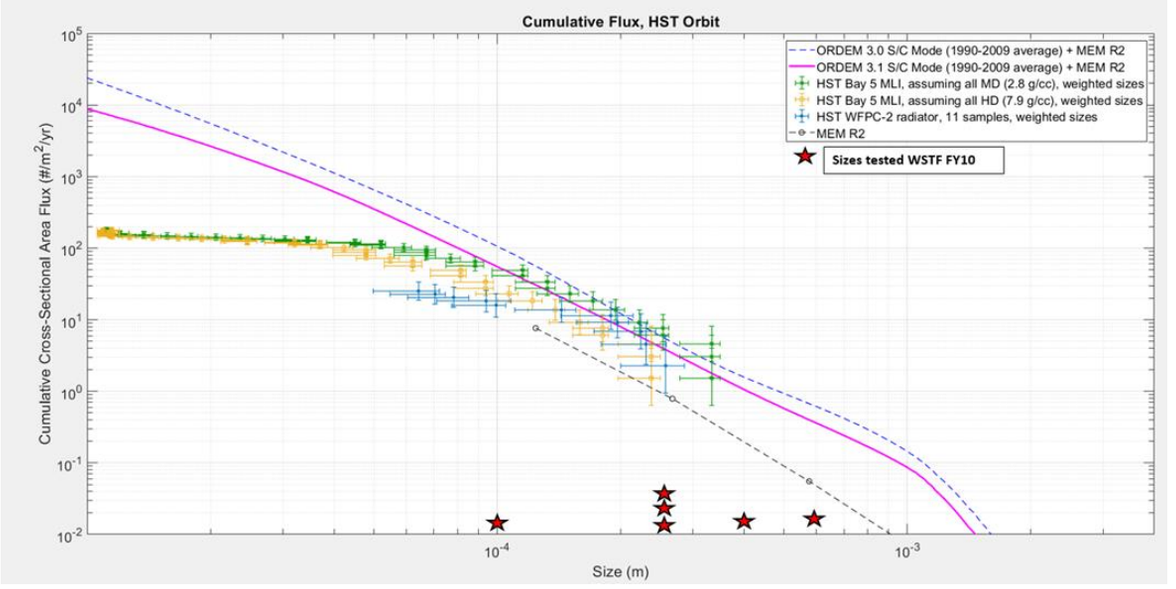

Fig. 17. ORDEM results of cumulative cross sectional area flux as a function of size at HST altitude. HST Bay 5 MLI medium and high density (MD, HD) are in green and yellow. Sizes in HVIT 2010 testing are labelled as red stars.

6 CONCLUSIONS

Analyzing impact features from returned spacecraft surfaces assisted in creating a model of the current orbital debris environment. Due to its 19-year duration and large area, the HST Bay 5 MLI panel provided a useful source of high-altitude impact data. In four 20×20 cm samples, a total of 550 impact features (through-holes and craters) were characterized using a digital microscope, backlighting, filtering, 3D imaging techniques, and FIB cutting/imaging. Craters on the panel dominated the through-holes at sizes less than 100 μm, for the panel thickness (127 μm). Relatively complex morphological phenomenon on through-hole features were observed instead of clean puncture holes, making determination of diameters difficult. A taxonomy of observed morphological features was defined and consistent measurements were recorded (from innermost diameter going outward). Though no impact features made it all the way through the 17-layer stack, impact features were observed in up to eight of the 17 layers, and changed size/shape through each layer. To verify overhead imagery and 3D feature profiles, FIB cross sections and matching corresponding areas allowed deeper insight into the morphology of the impact feature and verified the petaling phenomena. A generic damage equation was proposed and it was determined, using data from a 2010 WSTF test campaign, that the OTH measurement produced the least error when estimating feature diameters and predicting projectile size. After inverting the damage equation to interpret projectile size, a cumulative cross section area flux as a function of size at HST altitudes was created for the validation of ORDEM 3.1 modeling results. The results, pending an analysis of impactor chemistry to determine actual density, were in good agreement with the total MM and OD flux. With this work, the necessity is established to conduct further WSTF range testing, exploring the parameter space to a greater degree than was done in 2010. Data taken from the HST MLI Bay 5 panel is critical for continued ORDEM development and characterizing the small debris population; adding more samples to the dataset will provide greater understanding, reduce uncertainties of models, and provide a more accurate estimation of impactor parameters.

7 REFERENCES

1. Hörz, F., Messenger, S., Bernhard, R., *et al*., "Penetration Phenomena in Teflon and Aluminum Films using 50-3200 μm Glass Projectiles," Abstracts of the Lunar and Planetary Science Conference, Vol. 22: p. 591, 1991.
2. McKay, D.S. "Microparticle Impacts in Space: Results from Solar Max Satellite and Shuttle Witness Plate Inspections," NASA (SDIO Space Environmental Effects on Materials Workshop, Part 1; pp. 301-327, May 1989.
3. Herbert, M.K., McDonnell, J.A.M. "Morphological Classification of Impacts on the EURECA & Hubble Space Telescope Solar Arrays," Proceedings on the Second European Conference on Space Debris, ESOC, SP 393, May 1997.
4. Hörz, F., *et al.* "Dimensionally Scaled Penetration Experiments: Aluminum Targets and Glass Projectiles 50 μm to 3.2 mm in Diameter," International Journal of Impact Engineering, Vol. 15 No. 3, pp. 257-280, 1994.
5. Hörz, F., "Cratering and penetration experiments in aluminium and Teflon: Implications for space-exposed surfaces," Meteoritics and Planetary Sci. 47, No. 4: pp. 763-97, 2012.Gardner, D.J., Shrine, N.R.G., McDonnell, J.A.M. "Determination of Hypervelocity Impactor Size from Thin Target Spacecraft Penetrations," Proceedings on the Second European Conference on Space Debris, ESOC, SP 393, May 1997.
6. Matney, M., Manis, A., Anz-Meador, P., *et al*., "The NASA Orbital Debris Engineering Model 3.1: Development, Verification, and Validation," Paper presented at the 1st International Orbital Debris Conference, Sugar Land, TX, 9-12 December 2019.